

Phenomenology of α_s at intermediate energy: the quark-hadron duality approach

A. Courtoy^{*†}

IFPA, Inst. de Physique, Université de Liège, Belgium

INFN-LNF, Frascati, Italy

E-mail: aurore.courtoy@ulg.ac.be

In this contribution to the proceedings, we analyze the transition from perturbative and non-perturbative QCD embedded in the coupling constant. In the study of quark-hadron duality, we suggest that the realization of the latter is related to the inclusion of non-perturbative effects at the level of the coupling constant. The outcome of our analysis is a smooth transition from perturbative to non-perturbative QCD physics, embodied in the running of the coupling constant at intermediate scales. While our approach is purely perturbative, we compare our result to various non-perturbative schemes.

QCD-TNT-III-From quarks and gluons to hadronic matter: A bridge too far?,

2-6 September, 2013

European Centre for Theoretical Studies in Nuclear Physics and Related Areas (ECT), Villazzano, Trento (Italy)*

^{*}Speaker.

[†]This work was funded by the Belgian Fund F.R.S.-FNRS via the contract of Chargée de recherches.

1. Introduction

It is well established now that the QCD running coupling (effective charge) freezes in the deep infrared, pointing out the breakdown of perturbation theory at in the infrared region. This feature is associated to the transition towards non-perturbative QCD and, therefore, to confinement. In this context, the question of the applicability of quark-hadron duality naturally arises. Quark-hadron duality states that, in specific kinematical regimes, both the perturbative and non-perturbative stages arise almost ubiquitously, in the sense that the non-perturbative description follows the perturbative one. The knowledge of perturbative QCD can be used to calculate non-perturbative QCD physics observables [1]. However, when considering perturbative QCD observables at low scales, we implicitly face an interpretation problem. Higher terms in the perturbative expansion of that observable need be taken into account, by definition. Rephrasing, it gives: we are trying to make up for the perturbative to non-perturbative QCD physics transition in the perturbative analysis. We suggest that this phase transition can be fully included in the interpretation of the role of the running coupling constant at the scale of transition instead.

There exists, in Deep Inelastic processes, a dual description between low-energy and high-energy behavior of a same observable, *i.e.* the unpolarized structure functions. Bloom and Gilman observed a connection between the structure function $vW_2(v, Q^2)$ in the nucleon resonance region and that in the deep inelastic continuum [2]: the resonances are not a separate entity but are an intrinsic part of the scaling behavior of vW_2 . The meaning of duality is more intriguing when the equality between resonances and scaling happens at a same scale. It can be understood as a natural continuation of the perturbative to the non-perturbative representation. This context is hence suitable for studying the rôle of the running coupling constant at intermediate energies.

2. Quark-Hadron Duality in QCD

A quantitative definition of *global duality* is accomplished by comparing limited intervals defined according to the experimental data. Hence, we analyze the scaling results as a theoretical counterpart, or an output of perturbative QCD, in the same kinematical intervals and at the same scale Q^2 as the data for F_2 . It is easily realized that the ratio,

$$R^{\text{exp/th}}(Q^2) \equiv \frac{\int_{x_{\min}}^{x_{\max}} dx F_2^{\text{exp}}(x, Q^2)}{\int_{x_{\min}}^{x_{\max}} dx F_2^{\text{th}}(x, Q^2)} = 1 \quad , \quad (2.1)$$

if duality is fulfilled.¹

Duality is violated (the ratio (2.1) is not 1) when considering the fully perturbative expression, and is still violated after corrections by the target mass terms. One possible explanation for the apparent violation of duality is the lack of accuracy in the Parton Distribution Functions (PDF) parametrizations at large- x .² Therefore, the behavior of the nucleon structure functions in the resonance region needs to be addressed in detail in order to be able to discuss theoretical predictions

¹In the analysis of Ref. [5], we use, for F_2^{exp} , the data from JLab (Hall C, E94110) [6] reanalyzed (binning in Q^2 and x) as explained in [7] as well as the SLAC data [8].

²In our analysis, we use the MSTW08 set at NLO as initial parametrization [9]. We have checked that there were no significant discrepancies when using other sets.

in the limit $x \rightarrow 1$. In such a limit, terms containing powers of $\ln(1-z)$, z being the longitudinal variable in the evolution equations, that are present in the Wilson coefficient functions $B_{\text{NS}}^q(z)$ become large and have to be resummed, *i.e.* Large- x Resummation (LxR). Resummation was first introduced by linking this issue to the definition of the correct kinematical variable that determines the phase space for real gluon emission at large x . This was found to be $\tilde{W}^2 = Q^2(1-z)/z$, instead of Q^2 [3]. As a result, the argument of the strong coupling constant becomes z -dependent [4],

$$\alpha_s(Q^2) \rightarrow \alpha_s\left(Q^2 \frac{(1-z)}{z}\right) . \quad (2.2)$$

In this procedure, however, an ambiguity is introduced, related to the need of continuing the value of α_s for low values of its argument, *i.e.* for $z \rightarrow 1$. In Ref. [5], we have reinterpreted α_s for values of the scale in the infrared region. To do so, we investigated the effect induced by changing the argument of α_s on the behavior of the $\ln(1-z)$ -terms in the convolution with the coefficient function B_{NS} :

$$F_2^{NS}(x, Q^2) = xq(x, Q^2) + \frac{\alpha_s}{4\pi} \sum_q \int_x^1 dz B_{\text{NS}}^q(z) \frac{x}{z} q\left(\frac{x}{z}, Q^2\right) , \quad (2.3)$$

We resum those terms as

$$\ln(1-z) = \frac{1}{\alpha_{s,\text{LO}}(Q^2)} \int^{Q^2} d\ln Q^2 [\alpha_{s,\text{LO}}(Q^2(1-z)) - \alpha_{s,\text{LO}}(Q^2)] \equiv \ln_{\text{LxR}} , \quad (2.4)$$

including the complete z dependence of $\alpha_{s,\text{LO}}(\tilde{W}^2)$ to all logarithms. Using the ‘resummed’ F_2^{theo} in Eq. (2.1), the ratio R decreases substantially, even reaching values lower than 1. It is a consequence of the change of the argument of the running coupling constant. At fixed Q^2 , under integration over $x < z < 1$, the scale $Q^2 \times (1-z)/z$ is shifted and can reach low values, where the running of the coupling constant starts blowing up. At that stage, our analysis requires non-perturbative information.

In the light of quark-hadron duality, it is necessary to prevent the evolution from enhancing the scaling contribution over the resonances. We define the limit from which non-perturbative effects have to be accounted for by setting a maximum value for the longitudinal momentum fraction, z_{max} . Two distinct regions can be studied: the ‘‘running’’ behavior in $x < z < z_{\text{max}}$ and the ‘‘steady’’ behavior $z_{\text{max}} < z < 1$. Our definition of the maximum value for the argument of the running coupling follows from the realization of duality in the resonance region. The value z_{max} is reached at

$$R^{\text{exp/th}}(z_{\text{max}}, Q^2) = \frac{\int_{x_{\text{min}}}^{x_{\text{max}}} dx F_2^{\text{exp}}(x, Q^2)}{\int_{x_{\text{min}}}^{x_{\text{max}}} dx F_2^{NS, \text{Resum}}(x, z_{\text{max}}, Q^2)} = \frac{I^{\text{exp}}}{I^{\text{Resum}}} = 1 . \quad (2.5)$$

3. The Running Coupling Constant

The direct consequence of the previous Section is that duality is realized, within our assumptions, by allowing α_s to run from a minimal scale only. From that minimal scale downward, the

coupling constant does not run, it is frozen. This feature is illustrated on Fig. 1. We show the behavior of $\alpha_{s,\text{NLO}}(\text{scale})$ in the $\overline{\text{MS}}$ scheme and for the same value of $\Lambda_{\overline{\text{MS}},\text{MSTW}}^{\text{NLO}} = 0.402 \text{ GeV}$ used throughout our analysis. The theoretical errorband correspond to the extreme values of

$$\alpha_{s,\text{NLO}} \left(Q_i^2 \frac{(1 - z_{\text{max},i})}{z_{\text{max},i}} \right) , \quad (3.1)$$

i corresponds to the data points. Of course, we expect the transition from non-perturbative to perturbative to occur at one unique scale. The discrepancy between the 10 values we have obtained has to be understood as the resulting error propagation. The grey area represents the approximate frozen value of the coupling constant,

$$0.13 \leq \frac{\alpha_{s,\text{NLO}}(\text{scale} \rightarrow 0 \text{ GeV}^2)}{\pi} \leq 0.18 . \quad (3.2)$$

The solid blue curve represents the (mean value of the) coupling constant obtained from our analysis using inclusive electron scattering data at large x . The blue dashed curve represents the exact NLO solution for the running coupling constant in $\overline{\text{MS}}$ scheme. The grey area represents the region where the freezing occurs for JLab data, while the hatched area corresponds the freezing region determined from SLAC data. This error band represents the theoretical uncertainty in our analysis.

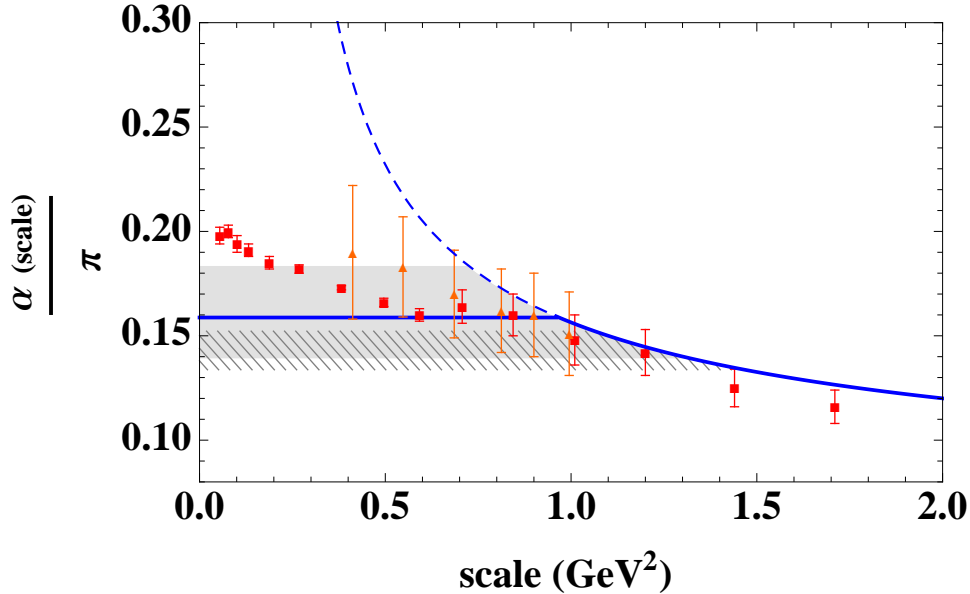


Figure 1: Extraction of α_s . See text.

In the figure we also report values from the extraction using polarized eP scattering data in Ref. [10, 11, 12]. These values represent the first extraction of an effective coupling in the IR region that was obtained by analyzing the data relevant for the study of the GDH sum rule. To extract the coupling constant, the $\overline{\text{MS}}$ expression of the Bjorken sum rule up to the 5th order in alpha (calculated in the $\overline{\text{MS}}$ scheme) was used. The red squares correspond to α_s extracted from Hall B CLAS EG1b, with statistical uncertainties; the orange triangles corresponds to Hall A E94010 / CLAS EG1a data, the uncertainty here contains both statistics and systematics. The agreement

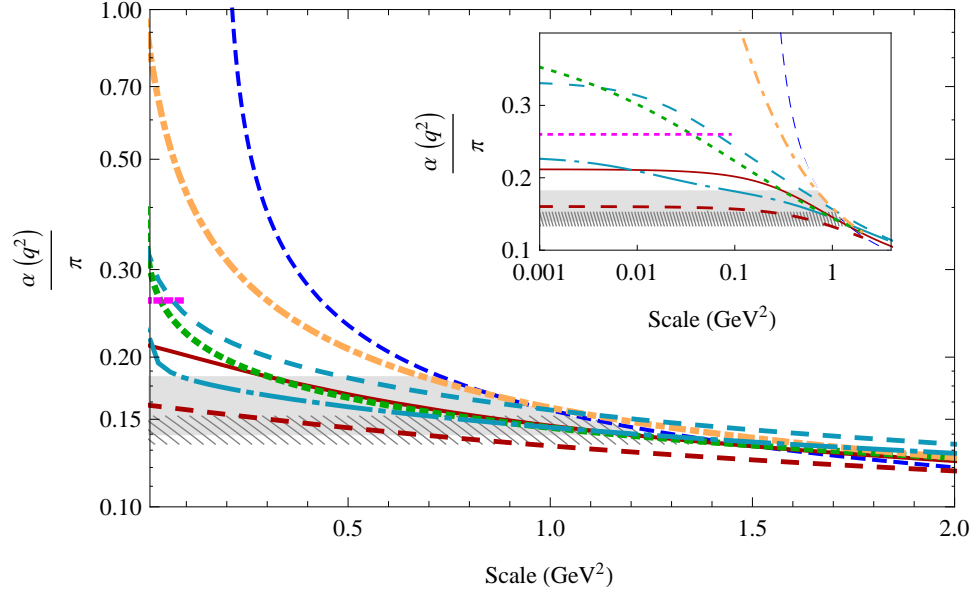


Figure 2: Comparison of the effective coupling constant. See text.

with our analysis, which is totally independent, is impressive. We notice, and it is probably one of the most important result of our analysis, that the transition from perturbative to non-perturbative QCD seems to occur around 1 GeV^2 .

At that stage, a comparison with fully non-perturbative effective charges and “modified pQCD” is noteworthy. It is shown in Fig. 2. The grey areas are as in Fig. 1 with $\Lambda_{\overline{\text{MS}},\text{MSTW}}^{\text{NLO}} = 0.402 \text{ GeV}$; the dashed blue curve is the exact NLO solution with the same Λ . The dotted-dashed orange curve corresponds to the result of Ref. [13], using the version (b) of their fit with $a = b = 1$. The latter analysis was performed in the MOM renormalization scheme. Though the β function does not depend on the scheme up to 2 loops, the definition of Λ varies from scheme to scheme. The comparison of the results is made possible using the relation, [14]

$$\Lambda_{\overline{\text{MS}}} = \frac{\Lambda_{\text{MOM}}}{3.334} \quad , \quad (3.3)$$

leading to the value of $\Lambda_{\overline{\text{MS}}}^{\text{Ref. [13]}} = (0.71/3.334) \text{ GeV} \sim 0.21 \text{ GeV}$. The value of $\alpha(0)$ is fixed to $8.915/N_c$. The red curves are variations of the effective charge of Ref. [15],

$$\frac{\alpha(Q^2)}{4\pi} = \left[\beta_0 \ln \left(\frac{Q^2 + \rho m^2(Q^2)}{\Lambda^2} \right) \right]^{-1} \quad (3.4)$$

with

$$m^2(Q^2) = m_0^2 \left[\ln \left(\frac{Q^2 + \rho m_0^2}{\Lambda^2} \right) / \ln \left(\frac{\rho m_0^2}{\Lambda^2} \right) \right]^{-1-\gamma} \quad ,$$

where (m_0^2, ρ, Λ) are parameters to be fixed. The solid red curve corresponds to the set $(m_0^2 = 0.3 \text{ GeV}^2, \rho = 1.7, \Lambda = 0.25 \text{ GeV})$, the dashed red curve to $(m_0^2 = 0.5 \text{ GeV}^2, \rho = 2., \Lambda = 0.25 \text{ GeV})$. This result is also obtained in the MOM scheme, the value of Λ turns out to be similar in both Fischer *et al.* and Cornwall’s approaches. The cyan curves correspond to two scenarios of the

effective charges of Ref. [16]. Their numerical solution is fitted by a functional form similar to Eq. (3.5). The 2 sets of parameters, corresponding to $m_0 = 500\text{MeV}$ (dashed-dotted curve) and 600 MeV (medium dashed curve), are then driven by the shape of the numerical solution. They are plotted here with the same $\Lambda_{\text{MOM}}^{n_f=0} = 300\text{ MeV}$ as in the publication, but for $n_f = 3$ for sake of comparison. Further investigation on comparison of schemes is needed. The short dashed green curves corresponds to Shirkov's analytic perturbative QCD to LO [17] with $\Lambda_{\overline{\text{MS}},\text{MSTW}}^{\text{LO}}$. The value of $\alpha(0)$ is fixed to $4\pi/\beta_0$. Finally, the pink curve is the freezing value of Ref. [18].

4. Conclusions

We report an interesting observation that the values of the coupling from different measurements/observables namely the GDH sum rule [12], and the large- x -DIS/resonance region based extractions, are in very good agreement. The extraction from the GDH sum rule, in a different (observable) scheme [10, 11], turns out to be in agreement with the prediction from AdS/CFT [19]. A comparison of our result in the $\overline{\text{MS}}$ scheme requires the extension to observable dependence [20] from scheme dependence. It will be studied in a future publication.

We have also compared our extraction to non-perturbative approaches. Notice that the extracted value for $\alpha_s(Q^2 < 1\text{GeV}^2)$ is only constrained by the integral in the resummed version of Eq. (2.3): no conclusion can be drawn on its value at $Q^2 = 0\text{GeV}^2$. While it is not possible to conclude on the value of $\alpha_s(0)$, we notice that it is possible to find sets of parameters for which the transition from perturbative to non-perturbative QCD occurs around 1 GeV^2 .

References

- [1] E. C. Poggio, H. R. Quinn and S. Weinberg, Phys. Rev. D **13** (1976) 1958.
- [2] E. D. Bloom and F. J. Gilman, Phys. Rev. Lett. **25** (1970) 1140; Phys. Rev. D **4** (1971) 2901.
- [3] D. Amati, A. Bassetto, M. Ciafaloni, G. Marchesini and G. Veneziano, Nucl. Phys. B **173** (1980) 429.
- [4] R. G. Roberts, Eur. Phys. J. C **10** (1999) 697 [hep-ph/9904317].
- [5] A. Courtoy and S. Liuti, Phys. Lett. B **726** (2013) 320 [arXiv:1302.4439 [hep-ph]].
- [6] Y. Liang *et al.* [Jefferson Lab Hall C E94-110 Collaboration], nucl-ex/0410027.
- [7] P. Monaghan, A. Accardi, M. E. Christy, C. E. Keppel, W. Melnitchouk and L. Zhu, Phys. Rev. Lett. **110** (2013) 152002 [arXiv:1209.4542 [nucl-ex]].
- [8] L. W. Whitlow, E. M. Riordan, S. Dasu, S. Rock and A. Bodek, Phys. Lett. B **282** (1992) 475.
- [9] A. D. Martin, W. J. Stirling, R. S. Thorne and G. Watt, Eur. Phys. J. C **63** (2009) 189 [arXiv:0901.0002 [hep-ph]].
- [10] A. Deur, V. Burkert, J. -P. Chen and W. Korsch, Phys. Lett. B **650** (2007) 244 [hep-ph/0509113].
- [11] A. Deur, V. Burkert, J. P. Chen and W. Korsch, Phys. Lett. B **665** (2008) 349 [arXiv:0803.4119 [hep-ph]].
- [12] A. Deur, Private Communication (2013).
- [13] C. S. Fischer and R. Alkofer, Phys. Rev. D **67** (2003) 094020 [hep-ph/0301094].

- [14] P. Boucaud, J. P. Leroy, J. Micheli, O. Pene and C. Roiesnel, *JHEP* **9810** (1998) 017 [hep-ph/9810322].
- [15] J. M. Cornwall, *Phys. Rev. D* **26** (1982) 1453.
- [16] A. C. Aguilar, D. Binosi, J. Papavassiliou and J. Rodriguez-Quintero, *Phys. Rev. D* **80** (2009) 085018 [arXiv:0906.2633 [hep-ph]].
- [17] D. V. Shirkov and I. L. Solovtsov, *Phys. Rev. Lett.* **79** (1997) 1209 [hep-ph/9704333].
- [18] A. C. Mattingly and P. M. Stevenson, *Phys. Rev. Lett.* **69** (1992) 1320 [hep-ph/9207228].
- [19] S. J. Brodsky, G. F. de Teramond and A. Deur, *Phys. Rev. D* **81** (2010) 096010 [arXiv:1002.3948 [hep-ph]].
- [20] G. Grunberg, *Phys. Lett. B* **95** (1980) 70 [Erratum-ibid. *B* **110** (1982) 501].